Apolipoprotein B-100 Conformation and Particle Surface Charge in Human LDL Subspecies: Implication for LDL Receptor Interaction†

Sissel Lund-Katz,*,‡ P. Michel Laplaud,§ Michael C. Phillips,‡ and M. John Chapman§

Department of Biochemistry, Allegheny University of the Health Sciences, MCP◆Hahnemann School of Medicine, 2900 Queen Lane, Philadelphia, Pennsylvania 19129, and National Institute for Health and Medical Research (INSERM) Unit 321, "Lipoproteins and Atherogenesis," Pavillon Benjamin Delessert, Hopital de la Pitie, F-75651 Paris Cedex 13, France

Received April 13, 1998; Revised Manuscript Received July 2, 1998

ABSTRACT: The plasma low-density lipoprotein (LDL) profile in coronary artery disease patients is characterized by a predominance of small, dense LDL. Small, dense LDL exhibit both high susceptibility to oxidation and low binding affinity for the LDL receptor, suggesting that these particles may be of elevated atherogenic potential. Here we examine whether the variation in biological function is due to differences in apo B-100 conformation that alter the interaction with the cellular LDL receptor. The microenvironments (pK_a) of Lys residues in apo B-100 in small, dense, intermediate, and light human LDL subspecies have been compared by ^{13}C NMR, and the net surface charge of these particles has been characterized. Relative to the total LDL fraction, small, dense, and light LDL subspecies have a decreased number of pK_a 8.9 Lys, while intermediate density LDL has a consistently higher number of pK_a 8.9 Lys. It follows that differences in protein conformation, as reflected in the Lys microenvironments, exist in the different LDL subspecies. Electrophoretic mobility measurements revealed that the light LDL subfractions exhibit a surface charge at pH 8.6 that is from −26 to −34e more negative than the intermediate density LDL subfraction. For the small, dense LDL particles the increments in negative charge range from −7 to −17e relative to the intermediate density LDL subfraction. These results suggest that differences in the conformation of apo B-100 and surface charge between LDL subspecies are major determinants of their catabolic fate. The lower number of pK_a 8.9 Lys leads to a reduction in binding of small, dense, and light LDL to the cellular LDL receptor and prolongs their plasma residence time, thereby elevating the atherogenicity of these particles. These data support the proposal that the intermediate LDL subspecies constitute the optimal ligand for the LDL receptor among human LDL particle subpopulations.

The low-density lipoprotein (LDL) particle is the principal carrier of cholesterol in human plasma and delivers exogenous cholesterol to cells by endocytosis via the LDL receptor (*1*). Elevated circulating levels of LDL have long been implicated in the premature development of atherosclerosis. Several studies have demonstrated that LDL consists of a continuum of particles that can be classified according to their physical and chemical properties; these include particle size, buoyant density, chemical composition, surface electrical charge, and hydrodynamic behavior [for reviews, see (*2*−*4*)]. Subpopulations of LDL have been identified by nondenaturing gradient gel electrophoresis and isolated by both differential ultracentrifugation (*5*) and equilibrium density gradient ultracentrifugation (*3*, *6*, *7*). Plasma LDL subspecies differ not only in their structural features but also in their metabolic characteristics (*8*−*11*) and in their oxidative behavior (*12*−*14*). Several studies have suggested that the net electric surface charge of lipoproteins might play an important role in their cellular interactions (*15*, *16*). This concept is supported by studies of modification of LDL by oxidation (*17*), acetylation (*18*), carbamylation (*19*), and glycation (*20*), each of which leads to an increase in the net negative charge of LDL particles. Highly negatively charged LDL particles are atherogenic because they are internalized by macrophage scavenger receptors which leads to foam cell formation and because they are no longer recognized by the LDL receptor.

The major cellular pathway for tissue catabolism of LDL particles is that of the LDL receptor (*21*). Nigon et al. (*9*) have evaluated the binding affinities and rates of degradation by the cellular LDL receptor pathway of discrete LDL subspecies from normolipidemic subjects; a homologous system of human U937 monocyte-like cells, which express large numbers of LDL receptors, was used. Both direct binding and displacement studies showed that LDL of intermediate density exhibited the highest binding affinity ($K_d \sim 5$ nM) and degradation rates. In comparison, light and dense LDL had lower affinities and were degraded at lower rates than the intermediate subspecies. In agreement with these findings, Jaakkola et al. (1989) (*8*) reported that mid-density LDL binds with high affinity to the LDL

† This work was supported by NIH Program Project Grant HL-22633 and by INSERM.

‡ MCP◆Hahnemann School of Medicine.

§ National Institute for Health and Medical Research (INSERM) Unit 321.

[1] Abbreviations: BSA, bovine serum albumin; CD, circular dichroism; δ, chemical shift; LDL, low-density lipoprotein; NMR, nuclear magnetic resonance; NOE, nuclear Overhauser effect; PI, phosphatidylinositol; *S*, surface potential; *V*, valence.

S0006-2960(98)00828-9 CCC: $15.00
Published on Web 08/28/1998

receptor and undergoes receptor-mediated uptake and degradation at greater rates than LDL of either lower or higher densities. The differences between LDL subspecies are significant because individuals with coronary artery disease have an increased prevalence of small, dense LDL particles (*22*). These particles also predominate in the LDL profile of subjects with non-insulin-dependent diabetes mellitus, familial dyslipidemic hypertension, and familial combined hyperlipidemia, conditions that are associated with coronary artery disease [for reviews, see (*2*) and (*22*)].

To examine if the variations in biological function between distinct LDL subpopulations arise from differences in apo B-100 conformation, we employed ^{13}C nuclear magnetic resonance (NMR) spectroscopy to compare the microenvironments of lysine residues in surface-exposed domains of apo B-100 in discrete LDL subspecies from normolipidemic subjects. The levels of active (p*K* 8.9) and normal (pK_a 10.5) lysines in apo B-100 of light (d. 1.022−1.029 g/mL), intermediate (d. 1.029−1.037 g/mL), and dense (d. 1.041−1.066 g/mL) LDL particles have been compared to that in total LDL (d. 1.024−1.050 g/mL) as a reference. The number of active (pK_a 8.9) lysine residues in apo B-100 of LDL particles of the intermediate subclass was found to be maximal, and distinct from those of LDL subspecies of lower and of higher density, in which lesser numbers of active lysines were detected. Since active (pK_a 8.9) lysine residues are specifically implicated in the interaction of apo B-100 with the LDL receptor, our data support the conclusion that apo B-100 in the intermediate LDL subspecies is in an optimal conformation for binding to this receptor. Electrophoretic measurements indicate that the net negative charge on the intermediate LDL particles is lower than that on dense and light LDL subspecies, respectively. Clearly then, the lower net negative charge of intermediate LDL is a consequence of the apo B-100 conformation on these particles which bind with relatively high affinity to the acidic ligand-binding domains of the LDL receptor (*23*).

EXPERIMENTAL PROCEDURES

Materials

Chemical Supplies. [^{14}C]Formaldehyde (40−60 Ci/mol) in distilled water was purchased from DuPont-New England Nuclear. Anionic contaminants were removed from the $H^{14}CHO$ by passage through a small Dowex 1-chloride column (*24*). [^{13}C]Formaldehyde (99% isotope enrichment as a 20% solution in water) was obtained from Cambridge Isotope Laboratories (Andover, MA). $NaCNBH_3$ from Aldrich (St. Louis, MO) was recrystallized from methylene chloride prior to use (*24*). Essentially fatty acid-free bovine serum albumin (BSA), ovalbumin, and dicaproyl-L-α-phosphatidylcholine were purchased from Sigma (St. Louis, MO). All other reagents were analytical grade.

Methods

Isolation of LDL and LDL Subspecies. Human LDL (d. 1.024−1.050 g/mL) was isolated from fresh plasma of healthy, normolipidemic donors by sequential ultracentrifugation as described previously (*3*, *25*). The plasma lipid and apoprotein levels in these subjects corresponded closely to those reported earlier (*3*). The method of isopycnic density gradient fractionation of LDL and the characterization of the derived subfractions have been outlined earlier (*3*). In brief, the nonprotein solvent density of dialyzed LDL samples was first raised to 1.040 g/mL by addition of solid KBr. Discontinuous density gradients were then constructed at ambient temperature in Ultraclear tubes (Beckman no. 344059) of a Beckman SW41 swinging-bucket rotor. Salt solutions were made up from NaCl and KBr, and their densitites were verified to the fourth decimal place with a precision densitometer (Model DMA40; Anton Paar, Gratz, Austria) at 15 °C. The gradients were centrifuged in a Sorvall OTD-50B or a Beckman L8-55 ultracentrifuge for 48 h at 15 °C and 40 000 rpm. To establish the density profile obtained upon completion of ultracentrifugation, control gradients containing NaCl/KBr solutions were fractionated identically, and their densities were determined at 15 °C as above. A calibration curve of solvent density as a function of volume was used to determine the density intervals of individual subfractions of LDL. Representative chemical compositions of the subfractions were determined and did not differ from those previously reported.

Circular Dichroism. The average secondary structure of apo B-100 in the LDL subspecies was monitored by circular dichroism (CD) spectroscopy using a Jasco J-41A spectropolarimeter calibrated with a 0.1% (w/v) *d*-10-camphorsulfonic acid solution as described previously (*26*). Briefly, the CD spectra were measured at 24 °C in a 0.1 cm path length quartz cell with a sample protein concentration of 50 μg/mL 5 mM phosphate buffer, pH 7.2. The percent α-helix in apo B-100 was calculated from the molar ellipticity at 222 nm using a mean residue weight of 113 (*27*).

Electrophoresis. The electrophoretic mobilities of LDL particles in barbital buffer (0.05 M, pH 8.6) were measured on Corning precast 1% agarose gels (Fisher Scientific, Malvern, PA) as described by Sparks and Phillips (*28*). The technique was adapted for the use of 1% agarose gels. The surface potential (*S*) was calculated from the equation $S = (V_e/P_e)6\pi n/D$ where V_e is the electrophoretic velocity [migration distance (cm)/time (30 min)], P_e is the electrophoretic potential [voltage applied (100 V)/gel distance (5.5 cm)], *n* is the coefficient of viscosity (0.0089 P), and *D* is the solvent dielectric constant (78.36). A detailed justification for the use of this equation is given by Sparks and Phillips (*28*). The net number of negative charges/LDL particle (valence, *V*) was also calculated as described (*28*).

The Stokes diameters of total LDL or LDL subfractions were measured using the polyacrylamide continuous gradient slab gel electrophoresis method. This was performed under the conditions reported by Nichols et al. (*29*), using a Pharmacia electrophoresis apparatus GE-2/4 loaded with PAA 2/16 gradient gels. Electrophoresis was carried out in a Tris−borate−EDTA buffer, pH 8.35, for 24 h at 15 °C and 125 V. Calibration was by means of a High Molecular Weight Calibration Kit (Pharmacia), of which only thyroglobulin and ferritin were retained, and by simultaneous use of latex particles with 380 Å diameter (Dow Chemical).

Labeling of LDL and LDL Subfractions. The reductive methylation procedure of Jentoft and Dearborn (*24*) was employed to introduce $^{13}CH_3$ groups into the amino groups of Lys residues of apo B-100 on the LDL particles. Conditions described previously (*30*) were used to convert from 10 to 30% of the Lys residues to the [^{13}C]dimethyl

derivative. There was no degradation of apo B-100 as monitored by electrophoresis on SDS−3% polyacrylamide/1% agarose gels.

NMR Measurements. ^{13}C NMR spectra at 126 MHz of the ^{13}C-labeled LDL preparations were obtained using a Bruker AM 500 spectrometer. The conditions employed to determine chemical shifts (δ) have been described previously (*30*). To obtain the intensities of the $(^{13}CH_3)_2$Lys resonances in the spectra of human LDL and its subfractions, a gated proton decoupler routine was employed to eliminate the nuclear Overhauser effect (NOE). The numbers of active and normal [^{13}C]dimethyl-Lys were determined as described previously (*31*).

Analysis of Phospholipid Composition. The average number of acidic phospholipid molecules in the LDL subspecies was determined by HPLC according to the method reported by Becart et al. (*32*) after extraction of total phospholipids as described by Bligh and Dyer (*33*). Briefly, a Beckman liquid chromatographic Gold system was used, and the detection was performed using a light-scattering detector Model DDL 21 (Eurosep Instruments, Cergy-Pontoise, France). Phospholipid subclasses were separated on a silica gel column (119 × 4 mm) "Supersher" Si60, 4 μm (Merck, Nogent-sur-Marne, France), using a binary gradient elution [solvent A: chloroform/methanol/ammonium hydroxide at 30% (50/19.5/0.5 v/v); solvent B: chloroform/methanol/water/ammonium hydroxide at 30% (60:34:5.5:0.5, v/v)]. In the light-scattering detector, the nebulization was performed at 70 °C and a pressure of 2 bar. The different phospholipid species were quantified by reference to a calibration curve which was constructed using a chloroform/methanol (1:1, v/v) solution containing given amounts of each phospholipid subclass and dicaproylphosphatidylcholine as an internal standard.

Other Analytical Procedures. Protein determination was carried out using the SDS−Lowry method of Markwell et al. (*34*), and phospholipid was monitored by phosphorus analysis (*35*).

RESULTS

Characterization of the Net Charge of LDL and LDL Subspecies. Experiments were conducted to characterize total LDL (d. 1.024−1.050 g/mL) and its subfractions from normolipidemic subjects to determine whether differences in apo B-100 conformation can account for their heterogeneous interaction with the LDL receptor (*9*). The net surface charges of the various LDL particles were determined quantitatively by electrophoresis of identical amounts of LDL protein on agarose gels. Staining the gels with Sudan Black B revealed the presence of a single band for each subfraction (data not shown). As shown in Table 1, the individual LDL subspecies from the center of the density gradient profile (i.e., LDL fractions 7, 8, and 9) have absolute electrophoretic mobilities up to 45% lower than those of the other LDL fractions, indicating that the intermediate fractions have lower net negative charge. This observation is in agreement with previously published electrophoretic mobilities (*3*, *36*). As seen in Table 1, LDL subfraction 8 (d. 1.033−1.0368/mL) in the intermediate density range has the lowest electrophoretic mobility, -0.30 ± 0.05 μm s^{-1} cm V^{-1}. Knowing the particle diameter from polyacrylamide gradient gel electrophoresis (Table 1), the valence, the surface potential, and the charge density of an LDL particle can be calculated. These parameters have values of -31 ± 5e, -5.8 ± 1.0 mV, and -678 ± 92 esu/cm^2, respectively, for fraction 8. The electrophoretic profiles of the other subfractions relative to fraction 8, the most positively charged particle, are illustrated in Figures 1 and 2A,B. The light LDL subfractions 3, 4, and 5 (density range 1.022−1.029 g/mL) have a negative surface charge that is from −26 to −34e more negative than fraction 8 (Figure 1). For the small, dense LDL particles (fractions 10−14), the increment in negative charge is approximately −7 to −17e relative to fraction 8 (Figure 1). A similar pattern is observed for the surface

Table 1: Comparison of Electrophoretic Mobilities and Particle Diameters of Total LDL and LDL Subfractions

fraction	average density[a] (g/mL)	diameter[b] (Å)	electrophoretic mobility[c] (μm s^{-1} cm V^{-1})
3	1.0215 ± 0.001	291 ± 2	0.55 ± 0.02
4	1.0234 ± 0.001	293 ± 6	0.52 ± 0.03
5	1.0260 ± 0.001	281 ± 2	0.49 ± 0.03
6	1.0286 ± 0.001	274 ± 3	0.43 ± 0.03
7	1.0314 ± 0.001	268 ± 2	0.31 ± 0.07
8	1.0343 ± 0.001	263 ± 2	0.30 ± 0.05
9	1.0372 ± 0.001	259 ± 2	0.36 ± 0.04
10	1.0409 ± 0.001	255 ± 2	0.39 ± 0.04
11	1.0451 ± 0.001	252 ± 2	0.44 ± 0.03
12	1.0502 ± 0.002	251 ± 3	0.42 ± 0.03
13	1.0580 ± 0.004	246 ± 6	0.44 ± 0.03
14	1.0660 ± 0.004	242 ± 3	0.45 ± 0.04
LDL	1.024−1.050	266 ± 5	0.31 ± 0.04

[a] Values are taken from Chapman et al. (*3*). Fractions 3−5 are designated large buoyant (light) LDL, fractions 7−9 are designated as intermediate density LDL, and fractions 10−14 are designated as small, dense LDL. [b] Values are the means ± SD of duplicate determinations on a series of subfractions from each of three individuals. Diameters were determined on polyacrylamide gradient gels as outlined under Methods. [c] Electrophoretic mobility (±SD) at pH 8.6 in 0.05 M barbital buffer.

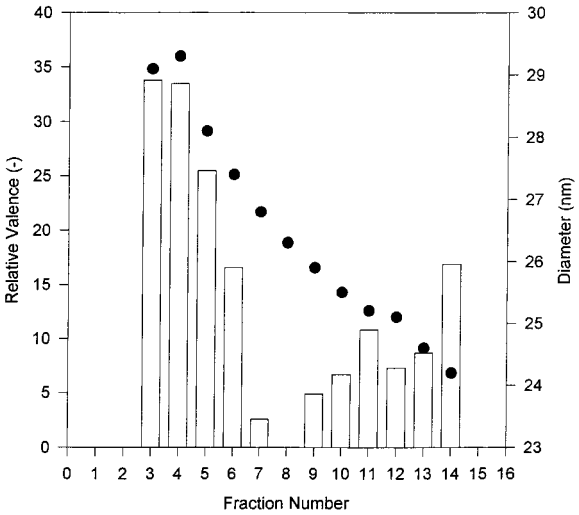

FIGURE 1: Net charge or valence (V) of light and of dense LDL subspecies relative to intermediate LDL subfraction 8 (d 1.0343 ± 0.001 g/mL). The charge characteristics of LDL density subfractions from fresh plasma of normolipidemic subjects (*3*) were obtained by measuring the electrophoretic mobilities of LDL particles on Corning precast 1% agarose gels at pH 8.6, as described by Sparks and Phillips (*28*). The least negatively charged intermediate LDL, subfraction 8, has a net negative charge (valence) of -31 ± 5e. Relative valence (open bars); LDL particle diameters in nanometers (●).

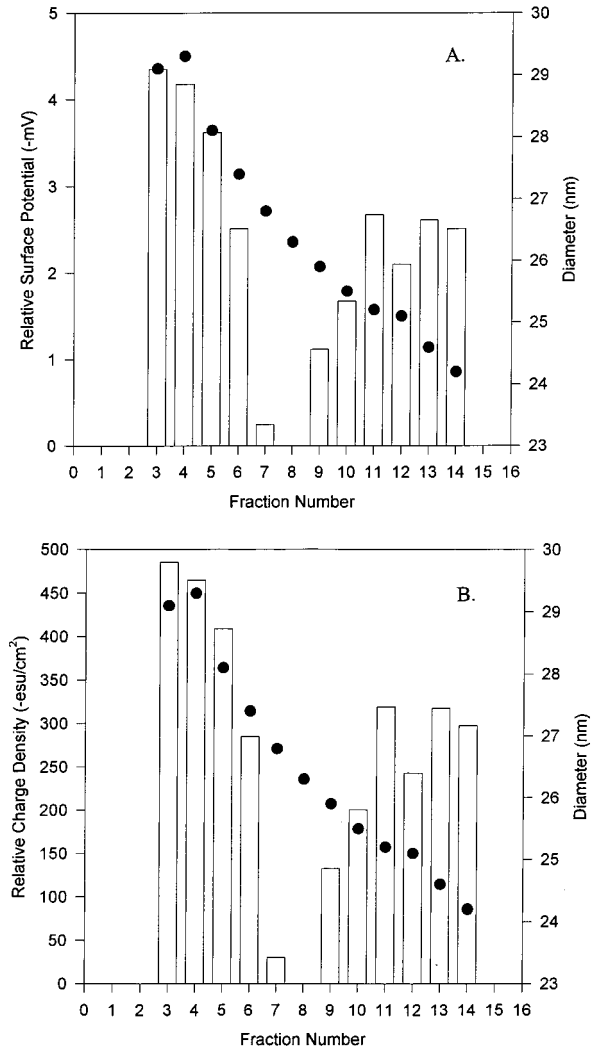

FIGURE 2: Surface potentials (*S*) and surface charge densities of light and dense LDL subspecies relative to intermediate LDL subfraction 8. (A) The surface potential *S* (open bars) of the LDL subfractions was calculated as described under Methods. Subfraction 8 has a surface potential value of -5.8 ± 1.0 mV. LDL particle diameters in nanometers (●). (B) The charge density (open bars) of the LDL subfractions was calculated as described under Methods. Subfraction 8 has a charge density value of -678 ± 92 esu/cm^2. LDL particle diameters in nanometers (●).

potential of the LDL subfractions where more negative values are apparent for the light and for small, dense LDL (Figure 2A). Comparison of the charge densities of the LDL subfractions shows that relative to fraction 8 both the lighter and the denser particles have values up to approximately 500 esu/cm^2 more negative than that of fraction 8 (Figure 2B). The above measurements of the variation in particle surface charge across LDL subfractions are in general agreement with a recent report (*36*). However, the electrophoretic mobilities of the LDL particles are higher in our study, and we attribute this to the use of a different electrophoresis system.

Circular Dichroism Measurements. Despite considerable differences in the electrophoretic behavior of the subclasses, the circular dichroism spectra between 184 and 260 nm of the LDL subclasses are similar, indicating that the average secondary structures of the apo B-100 molecule on the subspecies are similar ($40 \pm 5\%$ α-helical). Therefore, subtle differences in apo B-100 conformation due to variations in LDL particle size must be responsible for the observed dissimilarities in charge characteristics of these particles. The following two observations support this idea. (1) Fourier transform infrared spectroscopy suggests that there is slightly less apo B-100 β-strand content in small dense LDL (*37*). (2) The antigenicity of apo B-100 varies across LDL subspecies (*38*).

Effect of Phospholipid Composition on the Surface Charge of LDL and LDL Subfractions. To determine if a certain component in the LDL phospholipid fraction is responsible for the increase in negative charge reported above, the contents of acidic phospholipids in the surface of the LDL particles have been examined. The only acidic lipid detected was phosphatidylinositol (PI); the presence of increasing amounts of acidic PI molecules would be expected to augment the net negative charge and could therefore account for the charge difference between the subfractions. However, PI comprises $2.5 \pm 0.5\%$ of the phospholipid mass in all the LDL subfractions. This result shows that the fraction of PI is constant within experimental error for all the subfractions. Because the total number of phospholipid molecules per particle decreases as the LDL particles become smaller (*3*), the number of PI molecules per particle also progressively decreases as the particles became smaller. It follows, therefore, that the variation in number of PI molecules per particle is not the reason for the lower valence of LDL fraction 8 relative to the other LDL subfractions (Figure 1).

NMR Spectroscopy of LDL Subspecies. The microenvironments of lysine residues in surface-exposed domains of apo B-100 (*30*, *31*) in discrete LDL subspecies were examined to monitor the organization of the protein molecule. The ^{13}C NMR spectrum of human LDL is dominated by lipid resonances [cf. (39), (40)]. However, conversion of about 10% of the Lys residues to the $(^{13}CH_3)_2$Lys derivative gives rise to two well-defined resonances at δ 42.8 and 43.2 ppm (Figure 3). These chemical shifts are sensitive to pH, and titration shows that the dimethyl-Lys residues which resonate at $\delta = 42.8$ ppm at pH 7.6 have p$K_a = 10.5$. The dimethyl-Lys residues with $\delta = 43.2$ ppm at pH 7.6 have p$K_a = 8.9$ (*30*, *31*). These pK_a values apply to the unmodified lysine side chain because the titration characteristics of the dimethylated and unmethylated Lys ϵ-amino group are essentially identical. Integration of the $(^{13}CH_3)_2$Lys resonances gives the number of labeled Lys contributing to the signals, as previously reported (*30*, *31*).

Since there were insufficient amounts of subspecies 1−4 and 11−15 for study by NMR spectroscopy, we characterized the Lys residues in apo B-100 of fractions 5−10 (corresponding to the density range 1.0244−1.0435 g/mL); fractions 5−10 contain ∼95% of the protein mass of native LDL of *d* 1.024−1.050 (*3*, *9*). Consequently, the denser LDL subspecies (fractions 11 and 12) were excluded, thereby eliminating LDL subspecies containing small amounts of non-apo B-100 proteins (less than 5% of the protein moiety) (*3*, *4*, *9*).

From the NMR spectrum of LDL subfraction 8 in which 13% of the Lys are visualized by conversion to the dimethyl derivative (Figure 3B), there are about 26 dimethyl Lys with pK_a 8.9 and 19 with pK 10.5. The spectrum of the dimethyl-Lys residues in LDL subfraction 10 is shown in Figure 3C; this LDL subfraction labeled to 9% contains 12 pK_a 8.9 and

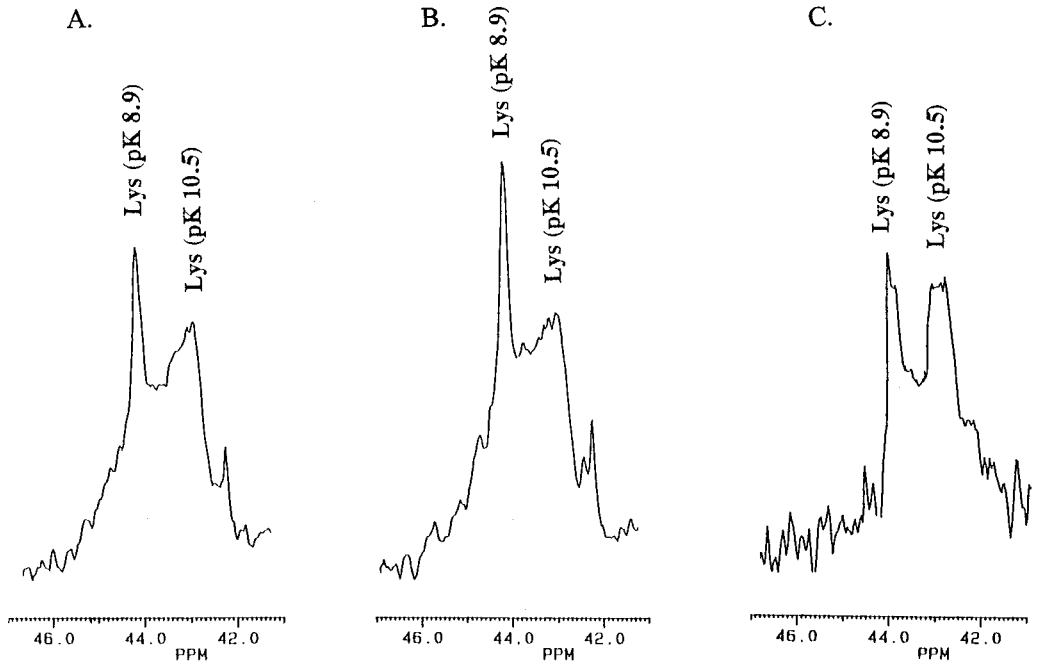

FIGURE 3: Proton-decoupled ^{13}C NMR spectra (126 MHz) of human LDL fractions. (A) $(^{13}CH_3)_2$Lys resonances of human LDL (d. 1.024−1.050 g/mL) from a normal subject in which 11.5% of the lysine residues were labeled (20.5 mg of protein in 1.5 mL of saline solution, 22 000 acquisitions). (B) $(^{13}CH_3)_2$Lys resonances of intermediate density LDL subfraction 8 (d. 1.0343 ± 0.001 g/mL) in which 13% of the lysine residues were labeled (10.6 mg of protein in 1.5 mL of saline solution, 30 500 acquisitions). (C) $(^{13}CH_3)_2$Lys resonances of small, dense LDL subfraction 10 (d. 1.0409 ± 0.001 g/mL) in which 9% of the lysine residues were labeled (5.6 mg of protein in 1.5 mL of saline solution, 43 500 acquisitions).

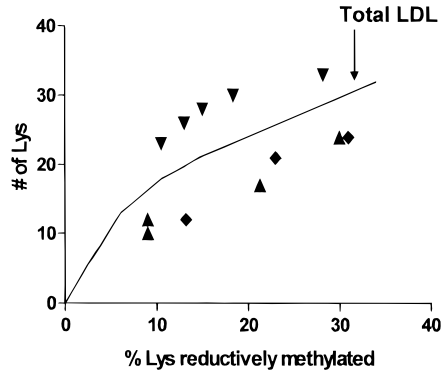

FIGURE 4: Numbers of pK_a 8.9 lysine residues in apo B-100 of human LDL fractions. The number of Lys was derived by integration of the $(^{13}CH_3)_2$Lys resonance at δ 43.2 ppm of NMR spectra of the type shown in Figure 3 and rounding to the nearest whole number. The nuclear Overhauser effect was suppressed so that the integrals reflect the number of ^{13}C nuclei contributing to each resonance; the integrals for each type of Lys are accurate to ±10%. The sizes of the pK_a 8.9 pools of dimethylated Lys of total LDL at different degrees of methylation are shown by the continuous line [data taken from ref (30)]. The symbols represent the numbers of pK_a 8.9 Lys in intermediate LDL subfraction 8 (▼), small, dense LDL (▲), and light LDL (◆).

21 pK_a 10.5 dimethyl-Lys. Comparison of Figure 3B and Figure 3C indicates that small, dense LDL (subfraction 10) has a decreased ratio of pK_a 8.9 to pK_a 10.5 Lys residues relative to intermediate subfraction 8. The numbers of pK_a 8.9 dimethyl-Lys in various preparations of LDL subfractions are compared in Figure 4; the size of the pK_a 8.9 pool of dimethyl-Lys of total LDL (d. 1.024−1.050 g/mL) at different degrees of methylation is shown by the continuous line. It is apparent that, relative to total LDL, the number of active (pK_a 8.9) lysine residues in apo B of intermediate density LDL is maximal, and distinct from those of LDL subspecies of lower and of higher density, in which lower numbers of active lysines are detected. Independent of the degree of ^{13}C labeling, there are approximately 10 fewer pK_a 8.9 Lys in the apo B-100 molecule present on the light and on the dense LDL particles relative to those of intermediate LDL (Figure 4). In summary, it is apparent that while the average secondary structure of apo B-100 (as reflected by the CD spectrum) is indistinguishable in the various LDL subspecies, differences in protein conformation, as reflected in the Lys microenvironments, exist in the various LDL subfractions.

DISCUSSION

LDL Particle Charge. The present investigation establishes, by quantitative measurements, the net negative charge on total LDL (d. 1.024−1.050 g/mL) and LDL subfractions. For total LDL, the value is −32e ± 3e at pH 8.6. This value shows a good correlation to the net charge of −58e (*41*), which is estimated from a tabulation of all charged groups per mole of LDL at its isoelectric point. Based on the chemical composition of LDL, an estimate of 1215 positively and 1273 negatively charged groups was proposed, leading to the net negative value of −58e. The present analysis of the net negative charge difference across the LDL subclass profile shows that the maximal charge difference across the subfractions is approximately 34e (Figure 1), a charge variation of about 53%. The observed heterogeneity in the charge characteristics of the LDL particles may arise from several distinct effects: (1) a direct effect due to dissimilarities in the relative proportions of various charged phospholipids between subspecies; (2) differences in the degrees of glycosylation or sialylation of the apo B-100; (3) a change in ionization of apo B-100 between subclasses, or from a combination of these effects.

Table 2: Contributions to the Net Surface Charge of LDL Particles

				apo B-100 conformation effects	
LDL fraction	particle valence (e)[a]	difference in valence from fraction 8 (e)	net PI charge contribution relative to fraction 8[b]	charge difference relative to fraction 8 from Lys pK_a shifts[c]	net charge contribution from other apo B-100 groups[d]
5	−57	−26	−3	3	−26
6	−48	−17	−2	3	−18
7	−34	−3	−1	0	−2
8	−31	0	0	0	0
9	−36	−5	2	3	−10
10	−38	−7	2	3	−12

[a] Calculated from electrophoretic mobilities (cf. Figure 1). [b] Derived from measured fraction of PL that is PI and assuming each PI molecule contributes 1 net charge to LDL particle. [c] The distribution of pK_a 8.9 and pK_a 10.5 Lys residues is taken from Figure 4 (see text). [d] Calculated for each LDL subfraction by subtracting the sum of the PI and Lys charge contribution from the difference in valence from fraction 8.

The electrophoretic and chemical characterization of the isolated LDL subspecies indicates that, although the acidic PI molecules contribute significantly to particle charge, charge variations across the subpopulation profile cannot be primarily accounted for by these lipids. Furthermore, although apo B-100 in LDL is sialylated, differences in sialic acid content are not responsible for the variations in charge properties across the spectrum of LDL subspecies (*36*). We have therefore focused on the variation in Lys ionization across the LDL subclass profile because this is a reflection of subtle changes in protein conformation.

To evaluate the contribution to the net negative surface charge from a change in the number of Lys with pK_a values of 10.5 and 8.9, we have used the Henderson−Hasselbalch equation (*42*) to define the effect of Lys ionization upon net negative particle surface charge. Using the Henderson−Hasselbalch equation, the ratio of ionized to un-ionized Lys can be calculated for pK_a 10.5 Lys at pH 8.6 to be $NH_3^+/NH_2 = 79:1$. From this, it is apparent that 1.25% of pK_a Lys 10.5 are un-ionized at pH 8.6. A similar calculation for pK_a 8.9 Lys at pH 8.6 shows that in this case, $NH_3^+/NH_2 = 2:1$ (i.e., one-third of the ϵ−amino groups are un-ionized). These calculations reveal that for every 100 Lys residues shifted from a normal microenvironment (pK_a 10.5) to an active microenvironment (pK_a 8.9), approximately one-third of the residues become deprotonated at pH 8.6. Thus, per 100 Lys shifted from a normal to an active microenvironment, there is a loss of 32 positive charges. These considerations can be applied to the individual LDL subspecies to estimate the contribution of changes in Lys pK_a values to net negative LDL surface charge.

Relative to the intermediate LDL subfractions 7 and 8, the light and dense subfractions are more negatively charged (Table 1, Figure 1). However, the light and the dense LDL fractions display a decreased number of active Lys (Figure 4) which, as outlined above, leads to a gain in positively charged Lys residues at pH 8.6. Therefore, this shift of Lys residues from pK_a 8.9 to pK_a 10.5 microenvironments tends to make the overall LDL particle more positively charged. The data in Figure 4 show that the ionization of about 10 Lys is modified by the differences in apo B-100 conformation arising from the increased or decreased particle sizes of the other LDL subfractions relative to fraction 8. It follows that the charge difference relative to fraction 8 arising from Lys pK_a shifts is +3e (Table 2). This charge difference is opposite in sign to the valences obtained from the electrophoretic mobilities which show that the other LDL subfractions are more negatively charged than fraction 8. Clearly, there are contributions from other charged groups on the LDL particle that explain the differences in subfraction net particle charge. As summarized in Table 2, variations in PI content do not explain the minimum in net negative charge occurring with fraction 8 because the number of PI molecules per particle progressively decreases as the particle size decreases. The changes in apo B-100 conformation alter the microenvironments of ionizable groups other than Lys with resultant changes in the net charge of the protein molecule. The calculations summarized in Table 2 show that this effect contributes −26e and −12e, respectively, to the charges of subfractions 5 and 10 compared to the contribution to the charge of fraction 8. While such changes in ionization have a significant effect on the net particle charge, these conformational effects are subtle given that there is a total of about 2500 charged groups on an LDL particle (*41*).

Interaction of Apo B-100 with the LDL Receptor. The concept that the creation of increasing numbers of active Lys (pK_a 8.9) leads to enhanced LDL receptor interaction is not consistent with a simple electrostatic interaction between the basic receptor binding domain of apo B-100 (*43*) and the acidic ligand-binding domain of the LDL receptor (*44*). As presented in this study, an increase in the number of active Lys (pK_a 8.9) reduces the number of positive charges on Lys at a physiological pH. The involvement of Lys in the binding of apo B-100 to the LDL receptor is apparent from the inhibition of binding of apo B-100 to the LDL receptor that is induced by chemical modification of this residue (*19*). The electrostatic interaction of domains containing basic Lys and Arg residues with acidic domains on the LDL receptor is thought to be critical to the binding process (*43*). However, the interaction is probably not simply electrostatic because reductive methylation of Lys does not remove the positive charge but does inhibit binding (*19*, *30*). Hydrogen bonding between the Lys ϵ-amino groups and sites on the receptor is likely to be important, and methylation reduces this possibility. The high-resolution structure of the ligand-binding repeat 5 of the LDL receptor also suggests that the interaction with ligand does not simply involve electrostatic interaction with acidic residues in the receptor (*45*); these acidic residues are buried to participate in calcium ion coordination. However, there is an exposed hydrophobic face that could participate in lipoprotein binding.

Nigon et al. (*9*) have clearly demonstrated that discrete LDL particle subspecies of defined physiochemical properties from normolipidemic subjects are heterogeneous in their

Table 3: Parameters Characterizing the Binding of LDL Subfractions to the LDL Receptor

fraction	K_d (nM)[a]	ΔG binding (−)(kcal/mol)[b]
5	8.35 ± 0.40	10.20 ± 0.03
6	5.71 ± 0.20	10.41 ± 0.06
7	5.24 ± 0.60	10.46 ± 0.06
8	4.57 ± 0.50	10.52 ± 0.06
9	7.20 ± 0.70	10.29 ± 0.05
10	6.87 ± 0.03	10.31 ± 0.01

[a] Equilibrium dissociation constants (K_d) for each subspecies were determined from the slopes of the Scatchard plots derived from measurements of the binding of LDL to the LDL receptor on U-937-monocyte-like cells [Nigon et al. (*9*)]. [b] The free energies of binding were calculated from the K_d values.

interaction with the LDL receptor on human U-937 cells, and that such heterogeneity involves not only receptor binding affinity at 4 °C but also the levels of cellular internalization and degradation at 37 °C. Analysis of the equilibrium dissociation constant, K_d, across the subpopulation profile (fractions 5−10) shows that the maximal difference in K_d is 3.8 nM, roughly a 50% difference (Table 3). The calculation of the free energies of binding (ΔG binding) for the various subclasses of LDL (Table 3) shows that fractions 5 and 8 differ in their ΔG binding by 0.3 kcal/mol. Such a ΔG value implies a subtle change in the nature of the binding. If altered polar interactions are involved, the 0.3 kcal/mol greater interaction energy of fraction 8 compared to fraction 5 is consistent with the presence of an additional salt-bridge or weak hydrogen bond between the apo B-100 molecule in fraction 8 and the LDL receptor molecule. On the other hand, if a nonpolar interaction is involved, a partial reduction in the exposure of a single methylene group to water would account for the 0.3 kcal/mol. Whatever its precise nature, the additional interaction must be a consequence of the difference in apo B-100 conformation induced by the ∼20 Å difference in particle diameter between LDL fractions 5 and 8.

Physiological Significance. The present data suggest that the variations in LDL particle diameters induce changes in the local conformation of the apo B-100 protein, resulting in altered ionization of basic and acidic amino acids. The least negatively charged LDL subspecies, 7 and 8, have conformations of the apo B-100 molecules which make them optimal ligands for binding to the LDL receptor. The lower receptor binding affinities of large, buoyant and of small, dense LDL subspecies (*9*) seem to be due at least in part to their increased net negative surface charge and reduced proportion of pK_a 8.9 Lys residues. Similarly, local conformational changes induced by the single amino acid substitution of Gln for Arg at position 3500 of apo B-100 in familial defective apo B-100 reduce the number of pK_a 8.9 Lys and disrupt the receptor-binding domain of apo B-100 (*31*). A change in the microenvironment of at least seven Lys residues from the basic microenvironment where they titrate with pK_a 8.9 to a microenvironment where they titrate normally with pK_a 10.5 is sufficient to reduce the binding of familial defective apo B-100 to the LDL receptor to 2−4% of the normal level (*46*). The variations in apo B-100 conformation across the LDL subfractions have relatively small effect on the LDL receptor affinity compared to that observed for the familial defective apo B-100 LDL particles. However, the reduction in the number of pK_a 8.9 residues in shifting from fraction 8 [which has the highest binding affinity (Table 3)] to either larger or smaller LDL particles is estimated to be only 3 (Table 2). The efficient removal of intermediate LDL from the circulation by the LDL receptor suggests that these particles are of lower atherogenic potential than either small, dense LDL (*47*) or large buoyant LDL (*48*). Both small, dense LDL and large, buoyant LDL have reduced clearance rates from the circulation because of their lower affinities for the LDL receptor. In addition, small, dense LDL exhibit efficient penetration of the arterial intima, high-affinity binding to arterial matrix components, and, finally, low resistance to oxidative stress which, in part, results from a deficient particle content of vitamin E (*14*, *49*).

In conclusion, structural and metabolic studies of physicochemically defined LDL subclasses clearly distinguish light, intermediate, and dense subpopulations on the basis of their biological functions and potential atherogenicity. The present results indicate that variations in the conformation of apo B-100 across the LDL subfraction profile give rise to metabolic differences, including the variations in binding affinity for the cellular LDL receptor.

ACKNOWLEDGMENT

We thank Dr. Jean-Louis Paul, Laboratoire de Biochimie, Hôpital Broussais, Paris, France, for kindly analyzing the phospholipid composition of the LDL subspecies. We thank Faye Baldwin, Sheila Benowitz, Margaret Nickel, and Fabienne Nigon for expert technical assistance.

REFERENCES

1. Goldstein, J. L., and Brown, M. S. (1977) *Annu. Rev. Biochem. 46*, 897−930.
2. Austin, M. A., Hokanson, J. E., and Brunzell, J. D. (1994) *Curr. Opin. Lipidol. 5*, 395−403.
3. Chapman, M. J., Laplaud, P. M., Luc, G., Forgez, P., Bruckert, E., Goulinet, S., and Lagrange, D. (1988) *J. Lipid Res. 29*, 442−458.
4. Chappey, B., Myara, I., Benoit, M.-O., Maziere, C., Maziere, J.-C., and Moatti, N. (1995) *Biochim. Biophys. Acta 1259*, 261−270.
5. Lee, D. M., and Alaupovic, P. (1970) *Biochemistry 9*, 2244−2252.
6. Shen, M. M. S., Krauss, R. M., Lindgren, F. T., and Forte, T. M. (1981) *J. Lipid Res. 22*, 236−244.
7. Lee, D. M., and Alaupovic, P. (1986) *Biochim. Biophys. Acta 879*, 126−133.
8. Jaakkola, O., Solakivi, T., Ylä-Herttuala, S., and Nikkari, T. (1989) *Biochim. Biophys. Acta 1005*, 118−122.
9. Nigon, F., Lesnik, P., Rouis, M., and Chapman, M. J. (1991) *J. Lipid Res. 32*, 1741−1753.
10. Zechner, R., Moser, R., and Kostner, G. M. (1986) *J. Lipid Res. 27*, 681−686.
11. Koren, E., Alaupovic, P., Lee, D. M., Dashti, N., Kloer, H. U., and Wen, G. (1987) *Biochemistry 26*, 2734−2740.
12. Tribble, D. L., Holl, L. G., Wood, P. D., and Krauss, R. M. (1992) *Atherosclerosis 93*, 189−199.
13. DeGraaf, J., Hendricks, J. C. M., Demacker, P. N. M., and Stalenhoef, A. F. H. (1993) *Arterioscler. Thromb. 13*, 712−719.
14. Dejager, S., Bruckert, E., and Chapman, M. J. (1993) *J. Lipid Res. 34*, 295−305.
15. Filipovic, I., and Buddecke, E. (1979) *Biochem. Biophys. Res. Commun. 88*, 485−490.
16. Nishida, H. I., Arai, H., and Nishida, T. (1993) *J. Biol. Chem. 268*, 16352−16360.

17. Henriksen, T., Mahoney, E. M., and Steinberg, D. (198). *Proc. Natl. Acad. Sci. U.S.A. 78,* 6499−6503.
18. Goldstein, J. L., Ho, Y. K., Basu, S. K., and Brown, M. S. (1979) *Proc. Natl. Acad. Sci. U.S.A. 76,* 333−337.
19. Weisgraber, K. H., Innerarity, T. L., and Mahley, R. W. (1978) *J. Biol. Chem. 253,* 9053−9062.
20. Witztum, J. L., Mahoney, E. M., Branks, M. J., Fisher, M., Elam, R., and Steinberg, D. (1982) *Diabetes 31,* 283−291.
21. Brown, M. S., Kovanen, P. T., and Goldstein, J. L. (1981) *Science 212,* 628−635.
22. Slyper, A. H. (1994) *JAMA 272,*305−308.
23. Brown, M. S., and Goldstein, J. L. (1986) *Science 232,* 1230−1237.
24. Jentoft, N., and Dearborn, D. G. (1983) *Methods Enzymol. 91,* 570−579.
25. Havel, R. J., Eder, H. A., and Bragdon, J. H. (1955) *J. Clin. Invest. 34,* 1345−1353.
26. Reijngoud, D.-J., and Phillips, M. C. (1984) *Biochemistry 23,* 726−734.
27. Morrisett, J. D., David, J. S. K., Pownall, H. J., and Gotto, A. M., Jr. (1973) *Biochemistry 12,* 1290−1299.
28. Sparks, D. L., and Phillips, M. C. (1992) *J. Lipid Res. 33,* 123−130.
29. Nichols, A. V., Krauss, R. M., and Musliner, T. A. (1986) *Methods Enzymol. 128,* 417−431.
30. Lund-Katz, S., Ibdah, J. A., Letizia, J. Y., Thomas, M. T., and Phillips, M. C. (1988) *J. Biol. Chem. 263,* 13831−13838.
31. Lund-Katz, S., Innerarity, T. L., Arnold, K. S., Curtiss, L. K., and Phillips, M. C. (1991) *J. Biol. Chem. 266,* 2701−2704.
32. Becart, J., Chevalier, C., and Biesse, J. P. (1990) *J. High-Resolut. Chromatogr. 13,* 126−129.
33. Bligh, E. G., and Dyer, W. J. (1959) *Can. J. Biochem. 37,* 911−917.
34. Markwell, M. A. K., Haas, S. M., Bieber, L. L., and Tolbert, N. E. (1978) *Anal. Biochem. 87,* 206−210.
35. Sokoloff, L., and Rothblat, G. H. (1974) *Proc. Soc. Exp. Biol. Med. 146,* 1166−1172.
36. LaBelle, M., Blanche, P. J., and Krauss, R. M. (1997) *J. Lipid Res. 38,* 690−700.
37. Tanfani, F., Galeazzi, T., Curatola, G., Bertoli, E., and Ferretti, G. (1997) *Biochem. J. 322,* 765−769.
38. Teng, B., Sniderman, A., Krauss, R. M., Kwiterovich, P. O., Milne, R. W., and Marcel, Y. L. (1985) *J. Biol. Chem. 260,* 5067−5072.
39. Hamilton, J. A., and Morrisett, J. D. (1986) *Methods Enzymol. 128,* 472−515.
40. Lund-Katz, S., and Phillips, M. C. (1986) *Biochemistry 25,* 1562−1568.
41. Margolis, S. (1969) in *Structural and Functional Aspects of Lipoproteins in Living Systems* (Tria, E., and Scanu, A. M., Eds.) pp 367−424, Academic Press, London and New York.
42. Segel, I. H. (1976) *Biochemical Calculations,* 2nd ed., p 32, John Wiley and Sons, New York.
43. Knott, T. J., Rall, S. C., Innerarity, T. L., Jacobson, S. F., Urdea, M. S., Levy-Wilson, B., Powell, L. M., Pease, R. J., Eddy, R., Nakai, H., Bryers, M., Priestly, L. M., Robertson, E., Rall, L. B., Betkholtz, C., Shows, T. B., Mahley, R. W., and Scott, J. (1985) *Science 230,* 37−43.
44. Goldstein, J. L., Brown, M. S., Anderson, R. G. W., Russell, D. W., and Schneider, W. J. (1985) *Annu. Rev. Cell Biol. 1,* 1−39.
45. Fass, D., Blacklow, S., Kim, P. S., and Berger, J. M. (1997) *Nature 388,* 691−693.
46. Innerarity, T. L., Mahley, R. W., Weisgraber, K. H., Bersot, T. P., Krauss, R. M., Vega, G. L., Grundy, S. M., Friedl, W., Davignon, J., and McCarthy, B. J. (1990) *J. Lipid Res. 31,* 1337−1349.
47. Austin, M. A., Breslow, J. L., Hennekens, C. H., Buring, J. I., Willet, W. C., and Krauss, R. M. (1988) *J. Am. Med. Assoc. 260,* 1917−1921.
48. Campos, H., Roedorer, G. O., Lussier-Cacan, S., Davignon, J., and Krauss, R. M. (1995) *Arterioscler. Thromb. Vasc. Biol. 15,* 1043−1048.
49. Goulinet, S., and Chapman, M. J. (1997) *Arterioscler. Thromb. Vasc. Biol. 17,* 786−796.

BI980828M